Proxies to describe ionospheric variability and heating rates of the upper atmosphere: current progress

C. Unglaub, Ch. Jacobi, G. Schmidtke, B. Nikutowski, R. Brunner

Summary

An updated version of the EUV-TEC proxy, describing the total primary ionisation of the upper atmosphere, is calculated from satellite-borne EUV measurements. Regional number densities of the background model atmosphere consisting of four major constituents are taken from the NRLMSISE-00 climatology. Furthermore, a first estimate of a global thermospheric heating rate is calculated from the absorbed energy. For the calculations the Lambert-Beer law is used to describe the decrease of the radiation along their way through the atmosphere. The EUV-TEC proxy is compared against the global mean total electron content (TEC), obtained from vertical TEC maps derived from GPS data. Strong correlations between these indices are found on different time scales. Results show that the EUV-TEC proxy describes the ionospheric variability better than the conventional solar index F10.7, especially at short time scales of days to weeks.

Zusammenfassung

Aus solaren EUV-Spektren wurde eine neue Version des EUV-TEC Proxys berechnet, der die primäre Gesamtionisation der oberen Atmosphäre beschreibt. Dafür wurden die regionalen Teilchendichten der einzelnen atmosphärischen Komponenten einer Modellatmosphäre berechnet. Des Weiteren wurde eine erste Abschätzung der mit der Energieabsorption verbundenen Erwärmungsraten durchgeführt. Zur Berechnung der atmosphärischen Absorption und Ionisation wurde das Gesetz von Lambert-Beer genutzt. Bei einem Vergleich von EUV-TEC mit dem globalen Gesamtelektronengehalt, der aus vertikalen Elektronenprofilen berechnet werden kann, offenbart sich eine starke Korrelation zwischen diesen Indizes auf unterschiedlichen Zeitskalen. Die Ergebnisse zeigen, dass der EUV-TEC Proxy die ionosphärische Variabilität besser beschreibt als der üblicherweise verwendete solare F10.7 Index.

1. Introduction

The EUV wavelength range is defined as the one between 10 nm and 120 nm (ISO, 2007). It is completely absorbed in the earth's atmosphere at altitudes above 50 km, so that it does not reach neither the troposphere nor the Earth's surface. The absorption occurs mainly in the upper atmosphere, i.e. in the thermosphere/ionosphere, and therefore EUV radiation is the most important energy source at altitudes above about 110 km. It interacts with the atmosphere in this region through photodissociation and photoionisation, the latter at wavelengths up to 102 nm, thereby leading to the

development of the planetary ionosphere. However, independent of the respective absorption mechanism EUV radiation finally causes heating of the upper atmosphere.

The total electron content (TEC) of the atmosphere is defined as the integrated electron density along a path under consideration. TEC depends on the solar EUV radiation and the composition of the atmosphere, which is in turn influenced by the EUV radiation variability (e.g., Maruyama, 2010). Thus, ionospheric changes mirror EUV changes. To determine TEC, the ionospheric influence of radio wave propagation paths may be used, because the ionospheric effect on the propagation velocity depends on the radio wave frequency and the ionospheric electron density integrated along the radio wave propagation path. Because GPS satellites emit two frequencies the total electron content along the line of sight between the GPS satellite and a ground-based receiver can be deduced. Subsequently this slant TEC may be converted into a vertical TEC applying an appropriate mapping function. Consequently, measured TEC can be defined as the height integrated electron density between the ground and the satellite orbit (Aggarwal, 2011).
The solar EUV radiation varies on different time scales, where the 11-year Schwabe sunspot cycle causes the primary decadal-scale irradiance variability and the Carrington rotation with an average period of 27 days causes the primary short-term variability. Consequences are strong changes of temperature, composition, density, electron density and ion content of the upper atmosphere. This can affect Low Earth Orbit (LEO) satellites and spacecraft through changes of the atmospheric drag, and may disturb communication and navigation signals (Woods, 2008).

Solar activity is often described by simple indices like F10.7, which is defined as the solar radio emission at a wavelength of 10.7 cm, although the primary factor that controls TEC variations and the variability of thermospheric density and temperature is the solar EUV radiation (Emmert et al., 2010, Maruyama, 2010). Furthermore, a nonlinear relationship between F10.7 and EUV fluxes is found (Liu, L., et al., 2011). Dudok de Wit and Bruinsma (2011) found that the EUV flux in the 26-34 nm band offers a better performance in the thermospheric density reconstruction than other indices like F10.7 or the MgII-index do. Therefore, especially under solar minimum conditions, conventional indices may not well describe the EUV radiation and there is a need for updated EUV indices to describe the ionospheric variability.

In this work we present an updated version of the EUV-TEC proxy (Unglaub et al., 2011), which is intended to explain solar induced ionospheric variability, because the ionospheric electron content is primarily determined by the direct photoionisation induced by the incident solar EUV radiation (Lean et al., 2011). The proxy thus describes ionospheric variability in response to the changing sun. The proxy may be used for space weather monitoring and ionospheric research. EUV-TEC is calculated from satellite-borne instruments measuring the EUV radiation considering the modified composition of the atmosphere which is caused by the EUV radiation. The proxy will be compared with F10.7 and the global mean TEC on different time scales to demonstrate that the EUV-TEC proxy describes the ionospheric variability better than conventional indices like F10.7.

Quasi independent of the absorption mechanism, the absorbed energy is finally transformed into heat, when the atmosphere is considered on a global scale and heat transport processes can be disregarded. Therefore, the calculated absorbed energy, which is a by-product of the EUV-TEC calculation, may be converted into a heating rate when taking into account the atmospheric composition. In the following, this heating rate, named EUV-THERM, is also presented.

2. EUV-TEC and EUV-THERM calculation

EUV spectra with a resolution of 1 nm are available from the Solar EUV Experiment (SEE) onboard the TIMED satellite (Woods et al., 2000, 2005) from February 2002 to date. We use version 10 level 3 products provided by LASP, University of Colorado. In addition, some available spectra from the SOLAR Auto-Calibrating EUV/UV Spectrometers (SolACES) Experiment (Schmidtke et al., 2006a, Nikutowski et al., 2010) are used for comparison.
For the calculation of EUV absorption and ionisation the regional thermospheric composition profiles are needed. Therefore a spherical model atmosphere is assumed around a spherical model Earth´s surface. The model atmosphere consists of the four major constituents O, N, O_2 and N_2 and reaches from the ground to an altitude of 1000 km with a resolution of 1 km. To obtain the regional thermospheric composition profiles, first a model sphere with 6370 km radius is assumed surrounded by 1000 spherical shells with 1 km distance representing the atmospheric layers. Then, the points of intersection between the radiation paths of the incoming EUV-radiation and the spherical shells are determined. Subsequently these intersection points are converted into geographical coordinates considering the declination. Thus, the regional thermospheric densities can be calculated by the NRLMSISE-00 model (Picone et al., 2002) for every particular atmospheric layer.

To obtain the EUV-TEC proxy, the primary ionisation is calculated for each atmospheric layer along the radiation paths using the Lambert-Beer law, whereby the required ionisation cross sections are taken from Metzger and Cook (1964) and Fenelly and Torr (1992) and the path lengths through each particular layer can be deduced from the intersection points between the radiation paths and the spherical shells. Integrating the primary ionisation over one day and multiplying with the area where the radiation impacts yields the total ion production rate per day in the atmosphere. Dividing the production rate by the surface of the earth, the EUV-TEC proxy is obtained representing the global mean ion production per day and m^2 in the atmosphere. In summary, the EUV-TEC calculation is similar to the one described in Unglaub et al. (2011), but there global mean atmospheric densities were considered, while now regional number density profiles are used.

The absorption of the EUV radiation causes heating of the upper atmosphere. Therefore, a first estimate of the heating rate of the atmosphere EUV-THERM can be deduced from the absorbed EUV energy by

$$\Delta T = \frac{\Delta E}{\sum_i n_i \cdot m_i \cdot c_{pi}}, \quad (1)$$

where i represents the respective constituents of the model atmosphere. ΔE is the absorbed energy, n_i is the number density, m_i is the mass and c_{pi} is the specific heat capacity of the respective gas i of the model atmosphere. ΔT is calculated for each intersection point between the radiation paths and the atmospheric layers, and subsequently a mean heating rate can be obtained, called EUV-THERM. The calculations are performed with a horizontal resolution of 220 km and a temporal resolution of 4 hours.

3. EUV-TEC results

Photoionisation rates may not be an appropriate dimension to describe electron densities locally, essentially because of the influence of dynamics. However, on a global scale a relatively strong correlation is expected. To check the quality of EUV-TEC as an ionospheric parameter, the proxy has been compared against a global daily mean TEC created from gridded vertical TEC maps recorded with the IGS tracking network (Hernandez-Pajares et al., 2009). To compare the indices, EUV-TEC, TEC, and F10.7 data were normalized by subtracting their mean value between July 2002 and June 2007 and dividing through their respective standard deviation. We chose this time period because EUV datasets from TIMED/SEE are available from February 2002 so a complete solar cycle is not available with a comparatively small data amount during solar maximum conditions that can be used for the normalization. This procedure also ensures that the peculiarities of the recent solar minimum are highlighted, since this time interval is not included in the data used for normalization. As a side effect, however, the average of the subsequently presented proxy data is not zero.

In Fig. 1 the time series of normalized EUV-TEC, normalized F10.7 and normalized global TEC are shown including the EUV-TEC data points based on SolACES measurements. The Figure essentially shows similar features like the one presented in Unglaub et al. (2011). For the SolACES points we apply the normalization of EUV-TEC calculated from TIMED/SEE measurements. There is generally good correspondence between these data points.

To study the solar influence on the atmosphere all data are uncorrected for the earth orbit effect. Comparing the three time series the annual pattern is well visible in both global TEC and EUV-TEC especially during low solar activity. This is, however not the case with the dynamically induced semiannual pattern, which is only visible in TEC.

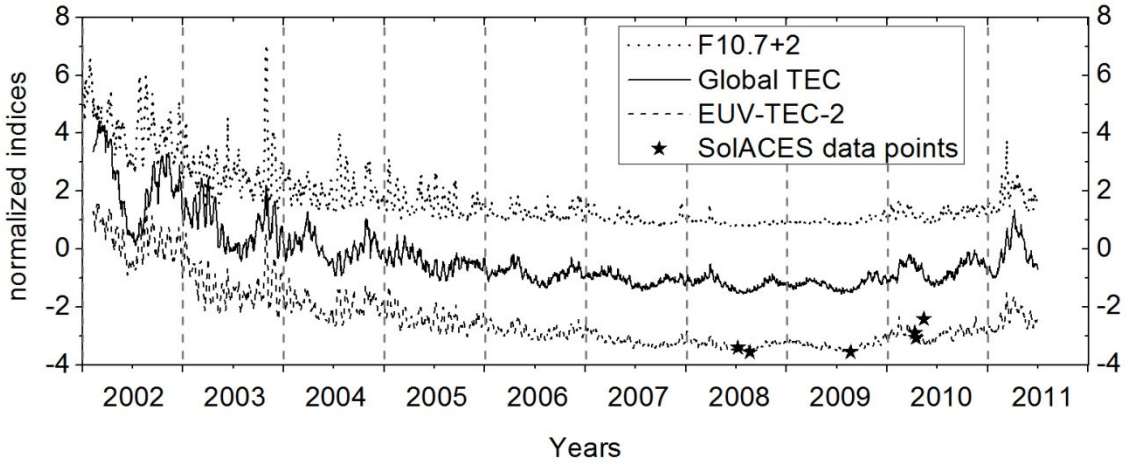

Fig. 1: Time series of the normalized EUV-TEC, global mean TEC and F10.7 from February 2002 to June 2011. The EUV-TEC data points based on SolACES measurements are shown as stars.

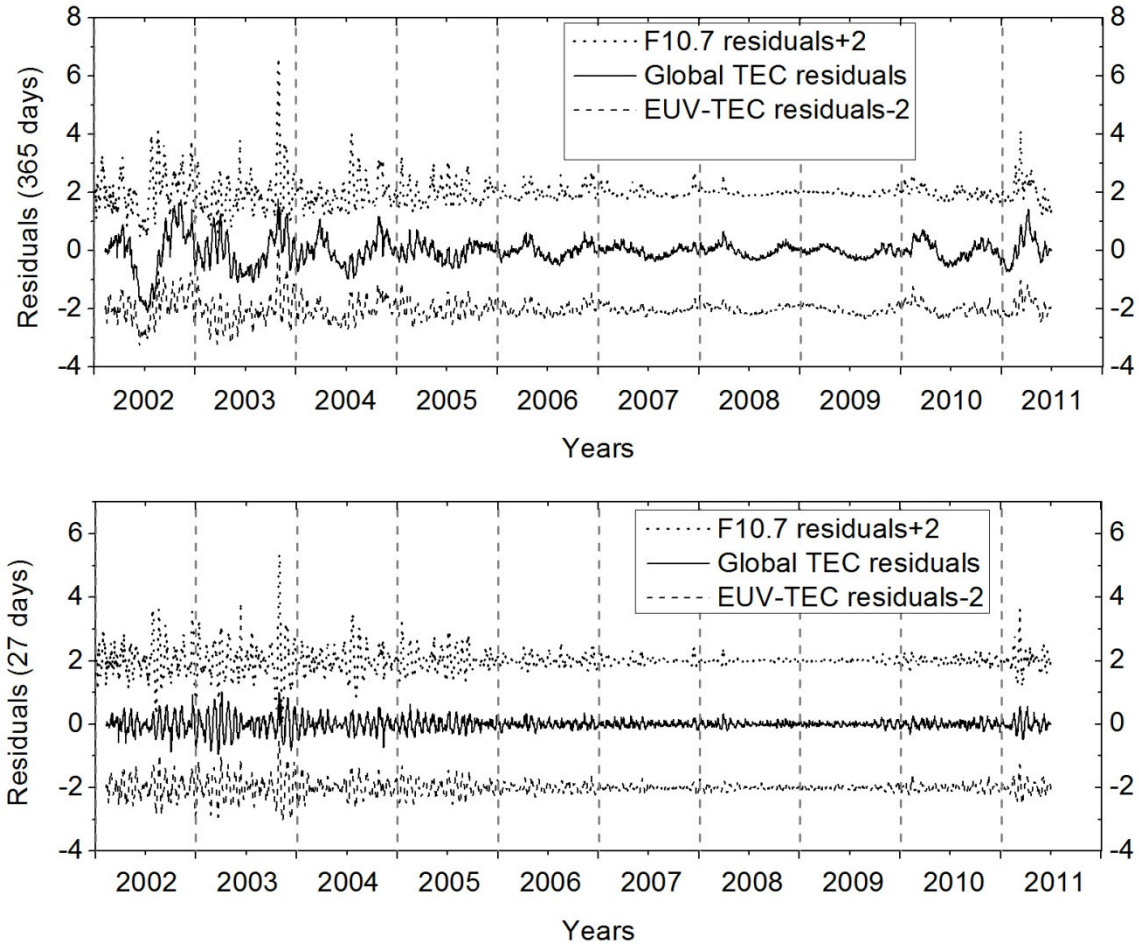

Fig. 2: Time series of residuals of the normalized EUV-TEC, global TEC and F10.7. The 365-days residuals are shown in the upper panel and the 27-day residuals are shown in the lower panel.

The seasonal pattern of EUV-TEC is mainly caused by the earth orbit effect where the earth is in perihelion at the beginning of January and in the aphelion at the beginning of July. Thus, EUV-TEC attains the largest values in the winter and the smallest values in summer. In addition to the earth orbit effect the seasonal pattern of global TEC shows a semiannual oscillation with maxima in spring and autumn. F10.7 shows a seasonal pattern which is caused by the earth orbit effect, too. But in contrast to EUV-TEC and global TEC, F10.7 attains nearly constant values during solar minimum conditions, thus showing a less marked seasonal pattern with a smaller amplitude than global TEC and EUV-TEC do. The dynamically induced semiannual oscillation of global TEC is described neither by EUV-TEC nor F10.7.

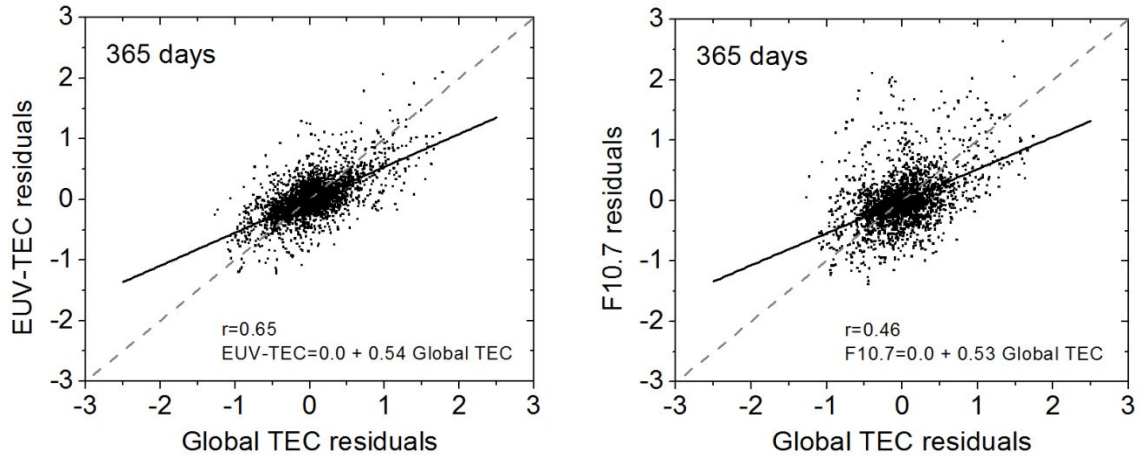

Fig. 3: Residuals after 365 day averaging. Left panel: EUV-TEC vs. global TEC, right panel: normalized F10.7 vs. global TEC.

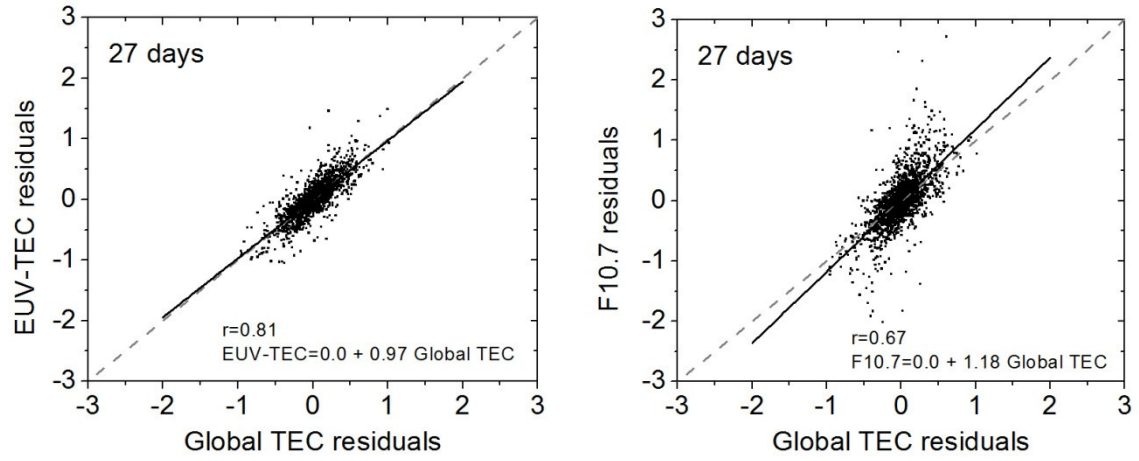

Fig. 4: As in Fig. 3, but for 27 days averaging.

For data from February 2002 to June 2011 there is a strong correlation of the EUV-TEC proxy and global TEC with a correlation coefficient of r=0.95, whereas the correlation between F10.7 and global TEC is weaker with a correlation coefficient of r=0.89. Thus, EUV-TEC describes the ionospheric variability, including long-term and

short-term variability better than F10.7 during 2002 to 2011. The strong correlations result from the 11-year Schwabe sunspot cycle, because all indices attain smaller values with decreasing solar activity.
To describe short-term variability, running averages over a defined time period (here 365 and 27 days) were calculated and the residuals were analysed. Fig. 2 shows the residuals of the normalized indices EUV-TEC, global TEC and F10.7 after subtracting their smoothed data over 365 days (upper panel) and 27 days (lower panel).

In the left panel of Fig. 3 the residuals (365 days) of EUV-TEC are shown vs. the residuals (365 days) of normalized global TEC. A significant correlation between these indices with a correlation coefficient of r=0.65 is obtained. For comparison, the correlation of the normalized residuals (365 days) of F10.7 vs. The normalized residuals (365 days) of global TEC is shown in the right panel of Fig. 3. There is a substantial weaker correlation than between the residuals of EUV-TEC and global TEC with a correlation coefficient of r=0.46. Thus, the ionospheric short-term TEC variability and its seasonal pattern are clearly better described by EUV-TEC than by F10.7. Because of the dynamical influence the seasonal pattern of global TEC has larger amplitudes than the seasonal pattern of both EUV-TEC and F10.7 has. This can be seen as well in Fig. 3 through the slope of the regression line smaller than 1.
In the left panel of Fig. 4 the 27 days residuals of EUV-TEC are shown vs. the 27 days residuals of normalized global TEC. There is a strong correlation with a correlation coefficient of r=0.81. The right panel of Fig. 4 shows the 27 days residuals of F10.7 vs. the 27 days residuals of global TEC. The correlation coefficient is r=0.67. Thus, also in this case the correlation between the residuals of F10.7 and global TEC is considerably weaker than the correlation between the residuals of EUV-TEC and global TEC. Furthermore, it can be seen in Fig. 4 that the amplitudes of the 27 days residuals of EUV-TEC and normalized global TEC are similar whereas the residuals of F10.7 slightly overestimate the residuals of global TEC. Thus, the ionospheric short-term variability up to 27 days, including the Carrington rotation is well described by the EUV radiation and thus can be better described by the EUV-TEC proxy than by the F10.7 index.

4. EUV-THERM: first results

From the EUV absorption rates a global mean thermospheric heating rate is calculated using the globally absorbed energy and the global thermospheric mass and composition by Eq. (1). To this end, we assume that the absorbed energy is finally and quasi-instantaneously transformed into heat, although without including dynamics and a detailed ionospheric model we cannot estimate, where this heating takes place. Thus a temperature signal constant over altitude is calculated as an index contributing to the analysis of the global energy budget.

The time series of the absorbed energy per day is shown in the upper panel of Fig. 5. As expected the absorbed energy time series shows the increasing values of the absorbed energy with increasing solar activity and the seasonal pattern caused by the

earth orbit effect. The corresponding time series of EUV-THERM is shown in the lower panel of Fig. 5. It was calculated using TIMED/SEE measurements in the wavelength range from 5 nm to 104 nm corresponding to the wavelength range where ionisation occurs (up to 102 nm), and thus the trend of the EUV-THERM proxy is very similar to this of EUV-TEC (see Fig. 1) and also following this of the absorbed energy. There is a very strong correlation between EUV-THERM and EUV-TEC and also between EUV-THERM and the absorbed energy with a correlation coefficient of r=0.99 in either case.
The very large heating rates of about 6000/14000 K/day during solar minimum/maximum conditions are not realistic for local heating, because we neglected dynamical effects and loss processes.

However, EUV-THERM is based on a physical model representing the solar based thermospheric variations. Because the thermosphere is influenced by both atmospheric (meteorological) and solar signals, EUV-THERM in comparison to some parameter describing total thermospheric variability like density trends (Emmert et al., 2009) can be used to distinguish between solar and meteorological .

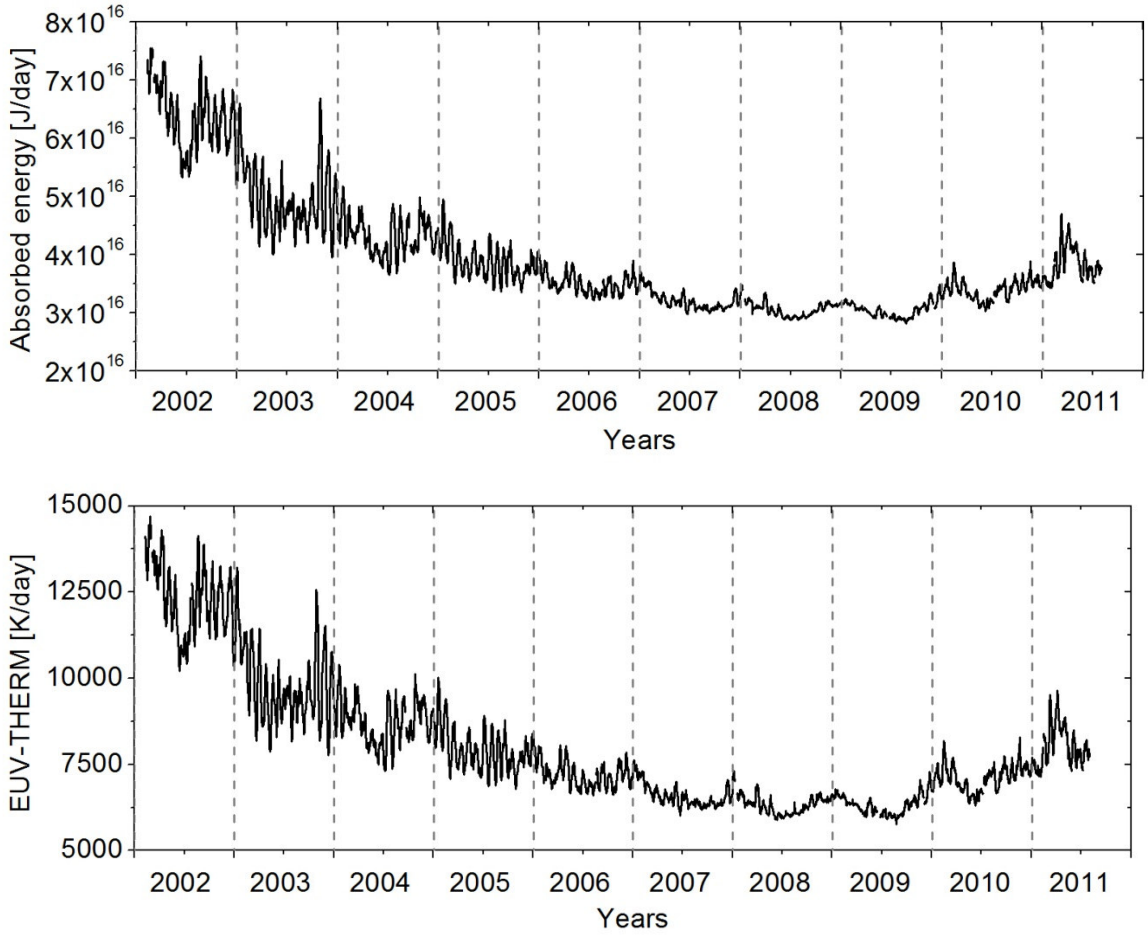

Fig. 5: Time series of the absorbed energy (upper panel) and the EUV-THERM index (lower panel) calculated with EUV measurements in the wavelength range from 5 nm to 104 nm.

5. Conclusions

From satellite-borne EUV measurements two proxies, EUV-TEC and EUV-THERM have been calculated. Here, as an update to earlier data presented in Unglaub et al. (2011) regional thermospheric composition profiles of the background atmosphere are taken from the NRLMSISE-00 climatology. The EUV-TEC proxy, representing a global mean photoionisation rate, describes the influence of the solar EUV irradiance variability on the ionosphere and thus can be considered as an ionospheric proxy useful for the analysis of space weather effects on the upper atmosphere. Comparisons of EUV-TEC with a global mean TEC created from vertical TEC maps show stronger correlations between these indices than between the conventional solar index F10.7 and global TEC especially on short time scales. On the whole, the EUV-TEC proxy performs better than F10.7 to describe ionospheric variability.

The EUV-THERM proxy, a global mean heating rate, is calculated from the absorbed energy in the wavelength range from 5 nm to 104 nm. It represents the solar induced thermospheric heating signal. The values are of the order of magnitude of 10^5 K/day. The proxy may be used to analyse solar effects on the thermosphere and to distinguish, in combination with other data, between solar and meteorological variability of the thermosphere.

Acknowledgements

This research has partly been performed in cooperation between IPM and Universität Leipzig. TIMED-SEE data has been provided by LASP, University of Colorado, through http://lasp.colorado.edu/see/see_data.html. TEC data has been provided by NASA through ftp://cddis.gsfc.nasa.gov/gps/products/ionex/. F10.7 indices have been provided by NGDC through ftp://ftp.ngdc.noaa.gov/STP/SOLAR_DATA/.

References

Aggarwal, M., 2011: TEC variability near northern EIA crest and comparison with IRI model, Adv. Space Res. 48, 1221–1231.

Emmert, J.T., Picone, J.M., Meier, R.R., 2009: Thermospheric global average density trends, 1967-2007, derived from orbits of 5000 near-Earth objects, Geophys. Res. Lett., 35, L05101, doi:10.1029/2007GL032809.

Emmert, J. T., Picone, J. M., 2010: Climatology of globally averaged thermospheric mass density, J. Geophys. Res., 115, A09326, doi:10.1029/2010JA015298.

Fennelly, J.A., Torr, D.G., 1992: Photoionization and photoabsorption cross sections of O, N2, O2 and N for aeronomic calculations, Atom. Data Nucl. Data Tables 51, 321–363.

Hernandez-Pajares, M., Juan, J.M., Sanz, J., Orus, R., Garcia-Rigo, A., Feltens, J., Komjathy, A., Schaer, S.C., Krankowski, A., 2009: The IGS VTEC maps: a reliable source of ionospheric information since 1998, J. Geod. 83, 263–275.

ISO, ISO 21348:2007(E), 2007: Space environment (natural and artificial) - Process for determining solar irradiances, ISO, 12 p.

Lean, J. L., Meier, R. R., Picone, J. M., Emmert J. T., 2011.: Ionospheric total electron content: Global and hemispheric climatology, J. Geophys. Res.,116, A10318, doi:10.1029/2011JA016567.

Liu, L., Chen, Y., Le, H., Kurkin, V.I., Polekh, N.M., Lee, C.-C., 2011: The ionosphere under extremely prolonged low solar activity, J. Geophys. Res., 116, A04320, doi:10.1029/2010JA016296.

Maruyama, T., 2010.: Solar proxies pertaining to empirical ionospheric total electron content models, J. Geophys. Res., 115, A04306, doi:10.1029/2009JA014890.

Metzger, P.H., Cook, G.R., 1964: A reinvestigation of the absorption cross sections of molecular oxygen in the 1050-1800 $\mathring{\text{A}}$ region, J. Quant. Spectrosc. Radiat. Transfer 4, 107–116.

Nikutowski, B., Brunner, R., Jacobi, Ch., Knecht, S., Ehrhardt, C., Schmidtke, G., 2010: SolACES spectrometers onboard the International Space Station (ISS), COSPAR 2010, Bremen, 18-25.7.

Picone, J.M., Hedin, A.E., Drob, D.P., 2002: NRLMSISE-00 empirical model of the atmosphere: statistical comparisons and scientific issues, J. Geophys. Res., 107, 1468, doi:10.1029/2002JA009430.

Schmidtke, G., Brunner, R., Eberhard, D., Halford, B., Klocke, U., Knothe, M., Konz, W., Riedel, W.-J., Wolf, H., 2006a: SOL–ACES: Auto-calibrating EUV/UV spectrometers for measurements onboard the International Space Station, Adv. Space Res., 37, 273-282.

Schmidtke, G., Fröhlich, C., Thuillier, G., 2006b: ISS-SOLAR: Total (TSI) and spectral (SSI) irradiance measurements, Adv. Space Res., 37, 255-264.

Unglaub, C., Jacobi Ch., Schmidtke G., Nikutowski B., Brunner R., 2011: EUV-TEC proxy to describe ionospheric variability using satellite-borne solar EUV measurements: first results, Adv. Space Res. 47, 1578–1584.

Woods, T. N., Bailey, S., Eparvier, F., Lawrence, G., Lean, J., McClintock, B., Roble, R., Rottmann, G. J., Solomon, S. C., Tobiska, W. K., White, O. R., 2000: TIMED Solar EUV Experiment, Phys. Chem. Earth (C), 25, 393–396.

Woods, T. N., Eparvier, F., Bailey, S., Chamberlin, P., Lean, J., Rottmann, G. J., Solomon, S. C., Tobiska, W. K., Woodraska, D. L., 2005: Solar EUV Experiment (SEE): Mission overview and first results, J. Geophys. Res., 110, A01312, doi:10.1029/2004JA010765.

Woods, T. N., 2008: Recent advances in observations and modeling of the solar ltraviolet and X-ray spectral irradiance. Advances in Space Research, 42:895–902.

Addresses of authors

C. Unglaub, Ch. Jacobi: Institut für Meteorologie, Universität Leipzig, Stephanstr. 3, 04104 Leipzig

G. Schmidtke, B. Nikutowski, R. Brunner: Fraunhofer-Institut für Physikalische Messtechnik (IPM), Heidenhofstraße 8, 79110 Freiburg